International Journal of Electrical, Electronic and Communication Sciences
ISSN: 2517-9438
Vol:1, No:2, 2007

Calibration of Time-Skew Error in a *M*-Channel Time-Interleaved Analog-to-Digital Converter

Yu-Sheng Lee, and Qi An

***Abstract*—**Offset mismatch, gain mismatch, and time-skew error between time-interleaved channels limit the performance of time-interleaved analog-to-digital converters (TIADC). This paper focused on the time-skew error. A new technique for calibrating time-skew error in M-channels TIADC is described, and simulation results are also presented.

***Keywords*—**Calibration, time-skew error, time-interleaved analog-to-digital converters.

I. Introduction

IT HAS BEEN known that time interleaving more than one ADC is a well-known technique used to increase the maximum sample rate [1]. Unfortunately, the performance of time-interleaved ADCs is sensitive to offset and gain mismatches as well as time-skew errors between the interleaved channels. The gain and offset errors in time-interleaved ADC's can be calibrated easily; the time-skew errors are difficult to process. In many cases it can become the dominant factor that limits the application of this architecture. To avoid the problem of the time-skew errors, the fractional delay filters was used in to calibration the time-skew errors in [2], but this method require the signal be oversampled with a factor of two or almost two compare to the Nyquist rate. Blind adaptive equalization of time-skew errors was proposed in [3], however the algorithms are quite computationally demanding, and it is very difficult to be implemented in circuits. Also, the multirate filter bank method based on the modeling of the analog analysis filters was given in [4], but the performance of this method can not performance well in all the Nyquist bandwidth due the modeling inaccuracies.

In this paper, a new technique based on the method of hybrid filterbank analog-to-digital converters is proposed. The transfer function of the reconstructing filters was derived; further, the impulse response of the transfer function was given in an analytical formula. Using the proposed method the time-skew errors can be calibrated as well as desired (in certain sense) by properly approximation the ideal reconstructing filters.

Manuscript received October 4, 2004. This work was supported by the National Natural Science Foundation of China Grant 10476028.

Y.-S. Lee and Q. An are with the Fast Electronics Lab, University of Science and Technology of China, Hefei Anhui 230026 China (phone: 086-0551-3606782; fax: 086-0551-3606782; email: yshli@ustc.edu).

II. Hybrid Analog/Digital Filter Banks

Consider the system in Fig.1, which we refer to as a hybrid analog/digital filter banks (HFB), or simply a filterbank ADC [5]. This system makes use of an analog analysis filter banks, uniform samplers and quantizers, upsamplers to retain the desired sampling rate $1/T_s$, and a digital synthesis filterbank. The sampling and quantization take place at the output of the analysis filters with the lower sampling frequency $1/T_1 = f_s/M$, since $T_1 = MT_s$, and the corresponding discrete-time frequency is $\omega_1 = \Omega T_1 = M\omega$. Ignoring the quantizations, The Fourier transform of the output signal can be written [2]:

$$Y\left(e^{j\omega}\right) = \frac{1}{T}\sum_{p=-\infty}^{\infty} X\left(j\frac{\omega}{T} - j\frac{2\pi p}{MT}\right)T_p\left(e^{j\omega}\right) \tag{1}$$

Where

$$T_p\left(e^{j\omega}\right) = \frac{1}{M}\sum_{m=0}^{M-1} F_m\left(e^{j\omega}\right)H_m\left(j\frac{\omega}{T} - j\frac{2\pi p}{MT}\right). \tag{2}$$

The input signal $x_c(t)$ is supposed to be band limited to π/T_s by external anti-alias filter. Then, within the interval $-\pi < \omega < \pi$, the output is:

$$Y\left(e^{j\omega}\right) = \sum_{p=-(M-1)}^{M-1} X\left(j\frac{\omega}{T} - j\frac{2\pi p}{MT}\right)T_p\left(e^{j\omega}\right). \tag{3}$$

Furthermore, considering $H_m(j\omega)$ band limited to π:

$$Y\left(e^{j\omega}\right) = \frac{1}{T}\sum_{p=0}^{M-1} X^S\left(j\frac{\omega}{T} - j\frac{2\pi p}{MT}\right)T_p^S\left(e^{j\omega}\right) \tag{4}$$

Where:

$$T_p^S\left(e^{j\omega}\right) = \frac{1}{M}\sum_{m=0}^{M-1} F_m\left(e^{j\omega}\right)H_m^S\left(j\frac{\omega}{T} - j\frac{2\pi p}{MT}\right) \tag{5}$$

And

$$X_m^S\left(j\Omega\right) = X\left(j\Omega\right) + X\left(j\Omega + j\frac{2\pi}{T}\right) \tag{6}$$

$$H_m^S\left(j\Omega\right) = H\left(j\Omega\right) + H\left(j\Omega + j\frac{2\pi}{T}\right) \tag{7}$$

Perfect reconstruction means that the output is simply a sampled, scaled and delayed version of the input. So, taking into account equation (4), the perfect reconstruction conditions

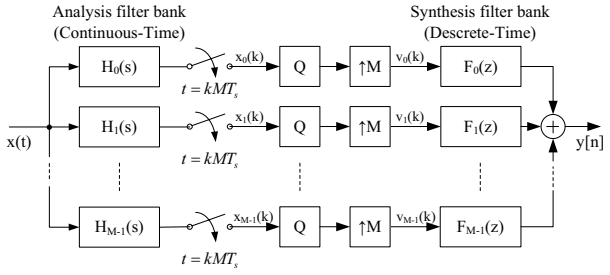

Fig. 2 TIADC output spectra: (a) without and (b) with calibration

are:

$$T_p^S\left(e^{j\omega}\right)=\begin{cases} ce^{-j\omega d}, & p=0 \\ 0, & p=1,2,\quad ,M-1. \end{cases} \tag{8}$$

$T_0^S(e^{j\omega})$, with $d\in\mathbb{R}$ being the filter bank's delay and $c\in\mathbb{R}$ a scale factor, indicates the HFB's gain and phase, represents the distortion function. $T_p^S(e^{j\omega})$, $p=1,\quad ,M-1$ are the aliasing functions since they show how the shifted, unwanted versions of the input are present in the output signal. Equation (4) contains *M* terms, so the perfect reconstruction conditions, as in (8) yields a linear system with *M* equations and *M* variables, the synthesis functions (as the analysis filter are supposed known). Then, perfect reconstruction has a unique solution for every frequency value considered. This idea is exploited by the hybrid filter bank method of TIADC Presented here.

If the analog analysis filters are selected according to

$$H_k\left(j\Omega\right)=e^{j\Omega t_k},\ k=0,1,\quad ,M-1. \tag{9}$$

Then, by sampling the output signals from the analysis filters in Fig.1. The subsequences $x_m\left(k\right)$ can be obtained as:

$$x_m\left(k\right)=x_c\left(kMT_s+t_m\right),\ m=0,1,\quad ,M-1. \tag{10}$$

The subsequences $x_m(k)$ are same as the discrete-time signals from the each channel of the TIADC. Thus the calibration of the time-skew error becomes to design the perfect reconstruction synthesis filter bank with the analysis filter bank be given in (9). This will be discussed in section III.

III. Design Reconstruction Filter for Calibration the Time-Skew Error

A. Derivation of the Principal Result

The system in Fig.1 is a perfect reconstruction (PR) system if equation (8) satisfied for some nonzero constant *c* and integer constant *d*. In the time domain, we have, in the PR case, $y(n)=cx(n-d)$. That is, with $c=1$, $y(n)$ is simply a shifted version of $x(n)$. Ignoring the delay *d*, we can thus retain $x_c(t)$ from $y(n)$, provided that the system in Fig.1 is PR system. Therefore, the PR condition in equation (8) has the following equivalent form for $\omega\in(-\pi,\pi)$:

$$\begin{cases} \sum_{m=0}^{M-1}F_m\left(\omega\right)H_m\left(\omega\right)=Me^{-j\omega d} \\ \sum_{m=0}^{M-1}F_m\left(\omega\right)H_m^S\left(\omega-2\pi p/M\right)=0,\quad p=1,\quad ,M-1. \end{cases} \tag{11}$$

For simplification, here we use $F_m(\omega)$ and $H_m(\omega)$ to represent $F_m(e^{j\omega})$ and $H_m(j\omega/T_s)$, respectively; and introduce variable d_k as $d_k=t_k/T_s$. It has been expatiated in section II that for every frequency $\omega\in(-\pi,\pi)$, the PR condition has a unique solution. Thus, the equation (10) must hold on each of the *M* subintervals $I_k=(-\pi+(k-1)\sigma,-\pi+k\sigma)$ for $k=1,2,\quad ,M$ where $\sigma=2\pi/M$. We show next that the solution of (11) is facilitated by considering these subintervals and we will arrive at a system which has to be solved only on the small interval I_1. Toward this end, we note from (10) that for $k=1,2,\quad ,M$

$$\omega\in I_k\Rightarrow\begin{cases} \sum_{m=0}^{M-1}F_m\left(\omega\right)H_m\left(\omega\right)=Me^{-j\omega d} \\ \sum_{m=0}^{M-1}F_m\left(\omega\right)H_m^S\left(\omega-2\pi p/M\right)=0, \\ \qquad p=1,\quad ,M-1. \end{cases} \tag{12}$$

These equations for the k th subinterval can be reduced to equations holding on I_1 by simple variable change, and then using the property of $H_m^S\left(\omega\right)$ in (7), we find that (12) have the form

$$\omega\in I_1\Rightarrow\begin{cases} \sum_{m=0}^{M-1}F_m\left(\omega+(k-1)\sigma\right)H_m\left(\omega+(k-1)\sigma\right) \\ \quad =Me^{-j(\omega+(k-1)\sigma)d},\ \text{for } v=k \\ \sum_{m=0}^{M-1}F_m\left(\omega+(k-1)\sigma\right)H_m^S\left(\omega+(v-1)\sigma\right) \\ \quad =0,\ \text{for } v=1,\quad ,k-1,k+1,\quad ,M-1. \end{cases} \tag{13}$$

Hence, we have a set of *M* equations for each of the *M* subintervals $I_k, k=1,\quad ,M$; the salient observation here is that for each subinterval the system is the same—only the position of $Me^{-j(\omega+(k-1)\sigma)d}$ changes as the subinterval is varied. For $\omega\in I_1$, equation (13) can be written more compactly in matrix as:

$$\mathbf{A}\left(d\right)\mathbf{E}\left(d,\omega\right)\mathbf{F}\left(\omega+(k-1)\sigma\right)=\mathbf{B}_k \tag{14}$$

Here:

$$\mathbf{A}(d)=\begin{bmatrix} 1 & 1 & \cdots & 1 \\ e^{jd_0\frac{2\pi}{M}} & e^{jd_1\frac{2\pi}{M}} & \cdots & e^{jd_{M-1}\frac{2\pi}{M}} \\ \vdots & \vdots & \ddots & \vdots \\ e^{jd_0(M-1)\frac{2\pi}{M}} & e^{jd_1(M-1)\frac{2\pi}{M}} & \cdots & e^{jd_{M-1}(M-1)\frac{2\pi}{M}} \end{bmatrix} \quad (15)$$

$$\mathbf{E}(d,\omega)=\begin{bmatrix} e^{j\omega d_0} & 0 & & 0 \\ 0 & e^{j\omega d_1} & & 0 \\ \vdots & \vdots & \ddots & \vdots \\ 0 & 0 & & e^{j\omega d_{M-1}} \end{bmatrix} \quad (16)$$

And

$$\mathbf{F}(\omega)=\begin{bmatrix} F_0(\omega) & F_1(\omega) & & F_{M-1}(\omega) \end{bmatrix}^T \quad (17)$$

$$B_k=\begin{bmatrix} 0 \\ \vdots \\ Me^{-j(\omega+(k-1)\sigma)d} \\ \vdots \\ 0 \end{bmatrix} \leftarrow k\text{th row} \quad (18)$$

For $\omega\in I_1$ and $k=1,\ \ ,M$, the matrix $\mathbf{A}(d)$ is a Vandermonde matrix [6] and matrix $\mathbf{E}(d,\omega)$ is a diagonal matrix. The necessary and sufficient condition for nosingularity of $\mathbf{A}(d)$ and $\mathbf{E}(d,\omega)$ is that $e^{jd_k 2\pi/M}$ be distinct, which is the same condition as $d_k\neq d_m+Mr, k\neq m, r\in\mathbb{Z}$. In practice, the condition of d_k can be satisfied without severe restriction, so there always exists a unique $F(\omega+(k-1)\sigma)$ satisfying (19) for fixed $k=1,\ \ ,M$.

$$\mathbf{F}(\omega+(k-1)\sigma)=\mathbf{E}^{-1}(d,\omega)\mathbf{A}^{-1}(d)\mathbf{B}_k \quad (19)$$

As *k* varies from 1 to *M*, $F(\omega+(k-1)\sigma)$ are determined on the successive subintervals $I_k, k=1,\ \ ,M$ through (19). In fact, if α_{mk} is the *mk*th element of matrix $\mathbf{A}(d)$, and use the inverse matrix of $\mathbf{E}(d,\omega)$ is $\mathbf{E}(d,-\omega)$, then:

$$F_{m-1}(\omega+(k-1)\sigma)=Me^{-j\omega(d+d_m)}e^{-j(k-1)\sigma d}\alpha_{mk} \quad (20)$$
$$1\le m,k\le M;\ \omega\in I_1.$$

Thus the terms of the inverse matrix $\mathbf{A}(d)$ effectively determined $F_0(\omega),\ \ ,F_{M-1}(\omega)$ on the full interval $\omega\in(-\pi,\pi)$.

B. Calculation of the Impulse Response

In this section, we calculate the impulse response of the discrete-time synthesis filters. By inverse discrete-time Fourier transformation,

$$\begin{aligned} f_m[n]&=\frac{1}{2\pi}\int_{-\pi}^{\pi}F_m(\omega)e^{j\omega n}d\omega \\ &=\frac{1}{2\pi}\sum_{k=1}^{M}\int_{I_k}F_m(\omega)e^{j\omega n}d\omega \end{aligned} \quad (21)$$

If we make the change of variable $\omega'=\omega-(k-1)\sigma$ in the *k*th integration, then using the equation (20), $f_m[n]$ can be written as:

$$f_m[n]=\frac{1}{2\pi}\sum_{k=1}^{M}\alpha_{mk}e^{jn(k-1)(k-1)2\pi/M}\int_{I_1}e^{-j\omega(d+d_m)}e^{j\omega n}d\omega \quad (22)$$

Using the inverse of Vandermonde matrix and the Lagrange interpolation polynomials in [6], then the impulse response $f_m[n]$ can be written as:

$$f_m[n]=\frac{M}{\pi}\frac{\prod_{i=0}^{M-1}\sin\left((n-d-d_i)\pi/M\right)}{(n-d-d_m)\prod_{\substack{i=0\\ i\neq m}}^{M-1}\sin\left((d_m-d_i)\pi/M\right)} \quad (22)$$

Equation (22) given the impulse response of the perfect reconstruction synthesis filters. Using these filters the periodic nonuniform samples from the TIADC can be reconstructed to uniformly sampled discrete-time signal. However, the impulse response of these filters is infinite in extent. To make the filter causal and realizable in practice with a finite-impulse response (FIR) structure, the natural choice is to truncate the filters about $d+d_m$ since the ideal $f_m[n]$ decays as $|d-d-d_m|$ increase. Further a windowing function $w_m[n]$ is also used which produce realizable FIR filters $\hat{f}_m[n]$ according to

$$f_m[n]=\begin{cases} f_m[n]w_m[n], & \text{for } |n-d-d_m|\le L \\ 0, & \text{for } |n-d-d_m|>L \end{cases} \quad (23)$$

These windowed filters will be of length 2*L* unless d_m is an integer, in which case it is trivial. The windowing function serves to smooth the time response. Without this windowing function a truncated filter's magnitude response is subject to *Gibbs phenomenon*, or large amounts of ripple. Frequency domain convolution serves to smooth out the ripple effects, although at the expense of an increased region of transition. This paper considers the Kaiser window, which has the design feature that the tradeoff between its transition region width and smoothing capability is somewhat controllable through its parameter β .

IV. Design Example and Simulation Results

To illustrate the usefulness of the proposed system, an example from [2] will be used. The continuous-time signal $x_c(t)$ is composed of the sum of four sinusoid terms with unit amplitude and respective frequencies of $F_s/16$, $F_s/8$, $3F_s/16$, and $F_s/4$. Five interleaved ADCs with respective

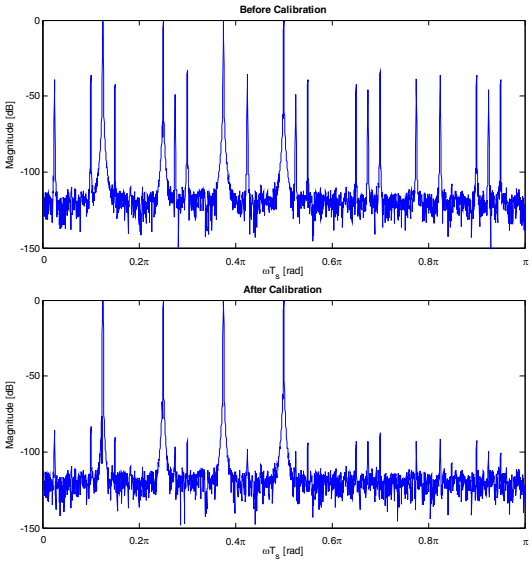

Fig. 2 TIADC output spectra: (a) without and (b) with calibration

d_k offsets $[0 \quad 0.96 \quad 2.02 \quad 2.99 \quad 4.03]$. This corresponds to respective time-skew errors of $[0 \quad -0.04T_s \quad 0.02T_s \quad -0.01T_s \quad 0.03T_s]$. Fig. 9(a) shows spectra before time-skew error calibration. The four tones that extending to 0dB are the only desired tones, all others have resulted from the imperfect sampling and are undesired. After using the calibration technique, the spectra are shown in Fig. 9(b).

Overall calibration performance is evaluated through examining the signal to noise-noise-distortion ration (SNDR) and spurious free dynamic range (SFDR). Before calibration the average SNDR is 30.5dB , and the average SFDR is 35.5dB . After calibration the average value of SNDR is 71.7dB ; and the average value of the SFDR is 85.8dB over $N = 5000$ samples, the parameter of Kaiser window $\beta = 4$. The reconstruction filters are 100th order. As shown in Fig. 3 and Fig. 4.

From the equation (20), we can known that the reconstructing filters are discontinuous in the points between any successive subintervals $I_k, k = 1, \quad , M$. So, the transition region takes the form of a small region of magnitude response inaccuracy centered about these points. This makes the reconstruction filters bank a poor calibration for signals occupying these frequencies (This can be seen from Fig. 3 and Fig. 4). Higher order synthesis filters will reduce the region of this error, as will decreasing the transition region through window design. Decreasing the transition region through windowing parameters is also of limited use due to the increase in undesirable ripple effects throughout a large portion of the spectrum, resulting in a poor reconstruction of the signals. But this tradeoff is acceptable for some applications where the accuracy is not seriously required. Further, in the applications where the accuracy is required, the error minimization method can be applied in these circumstances (This will be written in another paper).

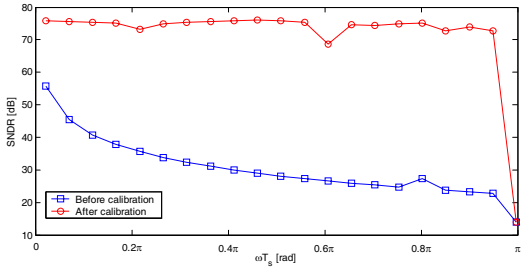

Fig. 3 the SNDR before and after calibration

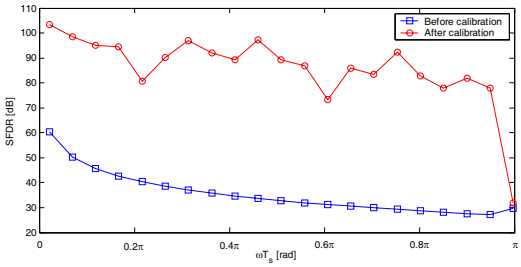

Fig. 4 the SFDR before and after calibration

V. Conclusion

This paper has described a new technique for calibration of the time-skew errors in time-interleaved analog-to-digital converters. The proposed technique based on the method of hybrid filter bank analog-to-digital converters. The transfer function of the reconstructing filters was derived; further, the impulse response of the transfer function was given in an analytical formula. Using the proposed method the time-skew errors can be calibrated as well as desired (in certain sense) by properly approximation the ideal reconstructing filters.

References

[1] W. C. Black Jr. and D. Hodges, "Time interleaved converter arrays," IEEE J. Solid-State Circuits, vol. SC-15, pp. 1022–1029, Dec. 1980.
[2] H. Johansson and P. Löwenborg, "Reconstruction of nonuniformly sampled bandlimited signals by means of digital fractional delay filters," IEEE Trans. Signal Processing, vol. 50, no. 11, pp. 2757-2767, Nov. 2002.
[3] J. Elbornsson, F. Gustafsson, and J. E. Eklund, "Blind adaptive equalization of mismatch errors in a time-interleaved A/D converter system," IEEE Transactions on Circuits and Systems I: Fundamental Theory and Applications, vol. 51, no.1, pp. 151-158, Jan., 2004.
[4] R. S. Prendergast, B. C. Levy, and P. J. Hurst, "Reconstruction of bandlimited periodic nonuniformly sampled signals through multirate filter banks," IEEE Trans. Circuits Syst. I, vol. 51, pp. 1612–1622, Aug. 2004.
[5] S. R. Velazquez, T. Q. Nguyen, and S. R. Broadstone, "Design of hybrid filter banks for analog/digital conversion," IEEE Trans. Signal Processing, vol. 46, pp. 956–967, Apr. 1998.
[6] M. E. A. El-Mikkawy, "Explicit inverse of a generalized vandermonde matrix," Applied Mathematics And Computation, vol. 146, pp. 643–651, Dec. 2003.